Cooperative grain boundary sliding and nanograin nucleation process in nanocrystalline, ultrafine-grained, and polycrystalline solids

S. V. Bobylev,[1,2] N. F. Morozov,[1,2] and I. A. Ovid'ko[1,2]

[1]*Institute of Problems of Mechanical Engineering, Russian Academy of Sciences, Bolshoj 61, Vasilievskii Ostrov, St. Petersburg 199178, Russia*

[2]*Department of Mathematics and Mechanics, St. Petersburg State University, St. Petersburg 198504, Russia*

(Received 19 May 2011; revised manuscript received 9 August 2011; published 14 September 2011)

A special physical mode of plastic deformation in nanocrystalline, ultrafine-grained, and polycrystalline solids is suggested and theoretically described. The mode represents the cooperative grain boundary (GB) sliding and nanoscale grain nucleation (occurring through stress-driven splitting and migration of GBs) process. It is theoretically revealed that, in certain ranges of parameters of the defect structure under consideration, the special deformation mode is more energetically favorable than both "pure" GB sliding and the previously examined [Bobylev *et al.*, Phys. Rev. Lett. **105**, 055504 (2010)] cooperative GB sliding and migration process. In addition, the special deformation mode enhances ductility of nanocrystalline and ultrafine-grained solids, and this enhancing effect is more pronounced compared to that of the cooperative GB sliding and migration process.

DOI: 10.1103/PhysRevB.84.094103 PACS number(s): 62.20.F−, 62.25.−g

I. INTRODUCTION

In recent years, a rapidly growing attention in physics of nanoscale plasticity has been paid to specific microscopic mechanisms/modes of plastic deformation in various nanocrystalline and ultrafine-grained solids; see, e.g.[1–15] In nanocrystalline solids, specific deformation modes operate due to the interface and nanoscale effects associated with structural peculiarities of these solids where the grain or crystallite size d is in the nanometer range, and the volume fraction occupied by grain boundaries (GBs) is extremely high; see reviews[16,17] and book.[18] For instance, GBs conduct plastic flow and serve as sources or sinks of lattice dislocations in nanocrystalline metals and ceramics.[16–21] In particular, GB sliding and other GB deformation modes effectively come into play in nanocrystalline solids with finest grains having typical sizes d lower than 10–20 nm in wide temperature ranges.[16–18] In addition, GB sliding serves as the dominant mode of superplastic deformation at elevated temperatures in nanocrystalline materials,[2,12,18,22,23] ultrafine-grained metals,[24,25] and polycrystals (with the microcrystalline structures characterized by grain sizes being of the order of 10 μm).[12,26]

GB sliding is strongly influenced by triple junctions of GBs, and this influence is of critical importance in nanocrystalline and ultrafine-grained solids where the amount of triple junctions is extremely large. In fact, triple junctions of GBs serve as obstacles for GB sliding, because direction of the plastic shear carried by GB sliding dramatically changes at such junctions. In general, GB sliding can be either accommodated or nonaccommodated at triple junctions, and this factor is significant for ductility of solids. When plastic flow of a solid involves nonaccommodated GB sliding processes, new defects—dislocations and disclination dipoles—are generated due to these processes at triple junctions of GBs.[27–29] The triple junction defects create high local stresses that can initiate cracks.[27–29] As a corollary, nonaccommodated GB sliding enhances brittle behavior of solids. It is contrasted with the situation where GB sliding is effectively accommodated through transformations of defects at triple junctions. As a result of such accommodating transformations, new defect configurations form that do not initiate cracks, and nanocrystalline as well as ultrafine-grained solids can show enhanced ductility and/or superplasticity.[18,24,30,31] With this role of accommodation of GB sliding in ductility of nanocrystalline and ultrafine-grained solids, it is highly interesting to reveal and describe the accommodating transformations of triple junction defects produced by GB sliding in such solids. The previous research in this area showed that incompatibility of GB sliding at triple junctions is effectively accommodated by "active" transformations of triple junction defects due to lattice dislocation emission from triple junctions, diffusion, and rotational deformation.[12,18,24,30,31] In addition, "passive" accommodation processes locally modify the GB structure but do not transform triple junction defects produced by GB sliding and thereby hardly influence generation of cracks in the stress fields of the defects. A typical "passive" accommodation mechanism represents local GB migration, which does not transform triple junction dislocations and disclination dipoles and is driven by extra GB curvature (produced by GB sliding) in nanocrystalline solids.[30–33] Recently a new physical deformation mode—the cooperative GB sliding and GB migration process—in nanocrystalline solids has been suggested and theoretically described.[34] This deformation mode involves stress-driven GB migration as an active accommodation mechanism for GB sliding. The theoretical representations[34] are supported by numerous experimental observations of GB migration and grain growth accompanying GB sliding in nanocrystalline metals and ceramics (for a review, see Ref. 35). At the same time, there are also experiments[36–42] and computer simulations[43–45] indicating structural transformation opposite to grain growth in nanocrystalline and polycrystalline solids under mechanical load. The transformation represents the deformation-induced nucleation of new microscopic and nanoscopic grains (nanograins) in nanocrystalline and polycrystalline solids. In doing so, the nanograin nucleation often occurs at GBs and their triple junctions.[39,43–45] (As for microscopic grains in plastically deformed polycrystals, they often nucleate at triple junctions as well.[39,40]) The main aim of this

paper is to suggest and theoretically describe the cooperative GB sliding and nanograin nucleation (CGBSNN) process as a new physical deformation mode involving the nanograin nucleation as an active accommodation mechanism for GB sliding. From a methodological viewpoint, the suggested description scheme serves as a generalization of the previous method[34] describing the cooperative GB sliding and GB migration process in nanocrystalline metals and ceramics.

II. GEOMETRY OF COOPERATIVE GRAIN BOUNDARY SLIDING AND NANOGRAIN NUCLEATION PROCESS

Let us consider the structural transformations associated with pure GB sliding and the CGBSNN process in a nanocrystalline solid (Fig. 1). The solid consists of nanoscale grains divided by GBs and is under a remote tensile load. A two-dimensional section of the solid is schematically shown in Fig. 1(a). First, we examine the situation where pure GB sliding occurs in a nanoscale configuration of grains and their GBs in the solid [Figs. 1(b) and 1(c)]. Following Refs. 27–29, GB disclination dipoles typically form due to GB sliding. For instance, Figs. 1(b) and 1(c) schematically show pure GB sliding, which occurs under the applied shear stress τ and transforms the initial configuration I of GBs [Fig. 1(b)] into configuration II [Fig. 1(c)]. Emission of lattice dislocations from triple junction [Fig. 1(c)] accommodates, in part, GB sliding incompatibility at the triple junction. In addition, GB sliding is accompanied by formation of a disclination dipole. More precisely, in the initial state [Fig. 1(b)], the triple junction A of high-angle GBs is supposed to be geometrically balanced. (There is no angle gap at the triple junction A, or, in other words, the sum of tilt misorientation angles at this triple junction is equal to zero.) As a result of GB sliding, configuration II is formed, and the angle gaps ω and $-\omega$ appear at the GB junctions A and C, respectively [Fig. 1(c)].[27–29] Here ω is the tilt misorientation of the GB AB assumed to be a symmetric tilt boundary.[27–29] In the theory of defects in solids, the junctions A and C with the angle gaps $\pm\omega$ represent wedge disclinations, which are characterized by the strengths $\pm\omega$[46,47] and form a dipole configuration. The disclination dipole AC is specified by its arm (the distance between the disclinations), which is equal to the magnitude x of the relative displacement of grains [Fig. 1(c)] and in fact characterizes local plastic strain carried by GB sliding in the vicinity of the triple junction under consideration. The disclination dipole AC represents a defect configuration whose stress field, in certain conditions, can initiate a triple junction crack[27–29] [Fig. 1(d)].

In parallel with plastic flow carried by GB sliding and other deformation modes, deformation-induced grain refinement often occurs in nano- and polycrystalline solids under mechanical load.[36–45] For instance, there are experimental observations of the formation of the nanocrystalline structure (nanocrystallization) in initially coarse-grained materials due to deformation processes.[36–39,42] Deformation-induced nanocrystallization is commonly treated to occur through continuous dislocation ensemble evolution resulting in consequent formation of dislocation subboundaries cells and high-angle grain boundaries.[18,36–38] In materials under dynamic load at cryogenic temperatures, grain refinement can also occur through nanoscale twin deformation.[41] In addition, recent

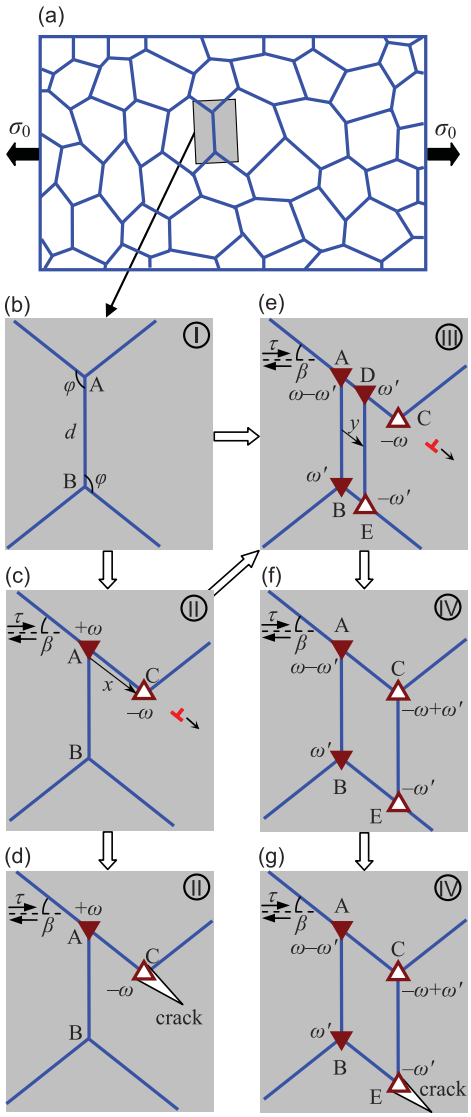

FIG. 1. (Color online) Grain boundary deformation processes in nanocrystalline specimen. (a) General view. (b) Initial configuration I of grain boundaries is presented. (c) Configuration II results from "pure" grain boundary sliding that produces a dipole of wedge disclinations A and C (small triangles). (d) Crack forms at the disclination dipole AC and grows into the grain interior. (e) Configuration III results from the cooperative grain boundary sliding and nanograin nucleation process. Grain boundary AB splits into immobile grain boundary (also called AB) and mobile grain boundary DE. The mobile boundary DE migrates under the shear stress and carries nanoscale plastic flow. As a result of the grain boundary splitting and migration, new disclinations D, B, and E are formed, and the strength of the disclination A changes. Value of ω' is equal to the tilt misorientation angle of the grain boundary DE. (f) When the disclinations D and E converge, the configuration IV forms, which contains the two disclination dipoles. (g) Crack forms at the disclination dipole BE and grows along a grain boundary fragment.

experiments[39] and computer simulations[44,45] have shown that nanograin nucleation effectively occurs through splitting and migration of GBs near their triple junctions in nano- and polycrystalline materials during their plastic deformation. In the theoretical paper,[48] it was suggested that the nanograin

nucleation (observed in the experiment[39] and computer simulations[44,45]) represents a special deformation mode occurring through stress-driven splitting and migration of GBs.

We think that both GB sliding and stress-driven nanograin nucleation can simultaneously occur as a cooperative stress-driven process, in which case defects created by GB sliding are, in part, accommodated by defects created by nanograin nucleation. In this context, the cooperative GB sliding and nanograin nucleation (CGBSNN) process serves as a special deformation mode, which, in certain ranges of characteristics of grain structures, is enhanced compared to pure GB sliding in nanocrystalline, ultrafine-grained, and polycrystalline solids. This view is supported by (1) our theoretical analysis (given below) and (2) the experimental observations[39–41] and computer simulations[44,45] of deformation-induced formation of new nanoscopic and microscopic grains at GBs and their triple junctions in polycrystalline and nanocrystalline solids during plastic deformation.

For illustrative purposes, we divide the CGBSNN process into the two stages. The first stage represents GB sliding, which occurs under the applied shear stress τ and transforms the initial configuration I of GBs [Fig. 1(b)] into configuration II [Fig. 1(c)]. As was discussed at the beginning of this section, the transformation in question is accompanied by the formation of the two wedge disclinations A and C that form a dipole configuration [Fig. 1(c)].

At the second stage of the considered process [Fig. 1(e)] the GB AB splits into the two GB fragments: the immobile fragment (also called AB) and the mobile GB fragment DE, which, for definiteness, is supposed to be a symmetric tilt boundary. The GB fragment DE under the action of shear stress τ moves over the distance y from its initial position AB [Fig. 1(e)]. Hereinafter, for simplicity, we consider the GB configuration with planar and parallel GBs AC and BE [in other terms, the angles φ in Fig. 1(b) are the same], in which case the length of the migrating GB does not change. In the spirit of the theory,[48,49] the splitting and migration of the GBs under consideration lead to the following transformations of the GB disclinations: (1) the disclination A characterized by the strength ω in its initial state [Fig. 1(c)] splits into the new disclination A with the strength $\omega - \omega'$ and the new disclination D having the strength ω' [Fig. 1(e)]; (2) a new disclination dipole BE with strengths $\pm\omega'$ is formed [Fig. 1(e)]. In doing so, the strength ω' is equal by magnitude to the misorientation angle of the new GB DE. The area ADEB represents a new nanograin whose formation is associated with migration of the GB DE and corresponding movement of disclination dipole DE that carries plastic deformation.

In the limiting situation, the CGBSNN process produces configuration IV [Fig. 1(f)] with the two disclination dipoles AC and BE, whose formation is due to convergence of the disclinations D and C. In addition, the generation of the disclination dipoles (playing the role of powerful stress sources) can initiate the formation of a crack releasing in part the stresses created by one of these dipoles [Fig. 1(g)].

Note that the CGBSNN process (Fig. 1) is divided into the two stages (the transformation of configuration I [Fig. 1(b)] into configuration II [Fig. 1(c)], and the transformation of configuration II [Fig. 1(c)] into configuration III [Fig. 1(e)]) for illustrative purposes. In reality, GB sliding and the new nanograin nucleation occur simultaneously as a cooperative stress-driven process (the transformation of configuration I [Fig. 1(b)] into configuration III [Fig. 1(e)]), in which case defects created by GB sliding are, in part, accommodated by defects created by the new nanograin nucleation.

So we have considered the geometric features of the CGBSNN process in a nanocrystalline specimen (Fig. 1). In general, a similar process can also occur at triple junctions of GBs in ultrafine- and coarse-grained polycrystals (in particular, during superplastic deformation of these materials at elevated temperatures) (Fig. 2). In doing so, its geometry

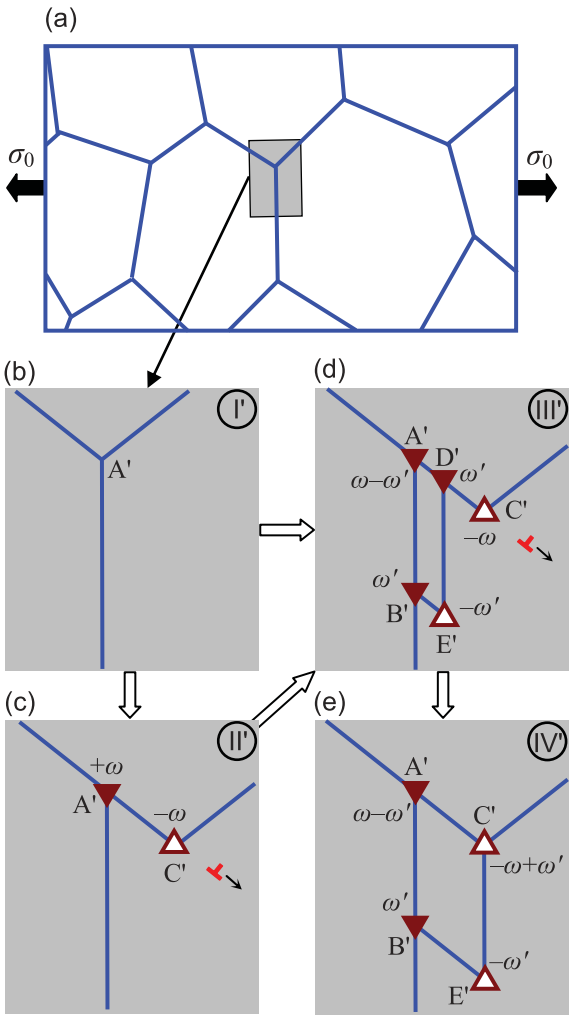

FIG. 2. (Color online) Grain boundary deformation processes in a coarse- or ultrafine-grained specimen. (a) General view. (b) Initial configuration I′ of grain boundaries is presented. (c) Configuration II′ results from "pure" grain boundary sliding. Dipole of wedge disclinations A′ and C′ (small triangles) is generated. (d) Configuration III′ results from the cooperative grain boundary sliding and nanograin nucleation process. Grain boundary A′B′ splits into immobile grain boundary (also called A′B′) and mobile grain boundary D′E′. The grain boundary D′E′ migrates, and this process is accompanied by the formation of the new grain boundary B′E′. Also, new disclinations D′, B′, and E′ are formed, and the strength of the disclination A′ changes due to the cooperative process under consideration. (e) When the disclinations D′ and E′ converge, the configuration IV′ forms, which contains two disclination dipoles.

(Fig. 2) is slightly different from that in nanocrystalline solids (Fig. 1). More precisely, the CGBSNN process in a polycrystal typically is accompanied by the formation of the two new GBs D′E′ and B′E′ of the new nanograin [Figs. 2(d) and 2(e)]. It is contrasted to the situation with the CGBSNN process in a nanocrystalline specimen (Fig. 1) where the new nanograin has the three preexistent GB and only one newly formed GB DE [Figs. 1(e) and 1(f)]. The difference in geometry between the CGBSNN processes (Figs. 1 and 2) weakly influences their energy characteristics (this will be analyzed in Sec. III). Therefore, hereinafter, for definiteness, we will focus our consideration on the CGBSNN process in nanocrystalline solids.

III. ENERGY CHARACTERISTICS OF COOPERATIVE GRAIN BOUNDARY SLIDING AND NANOGRAIN NUCLEATION PROCESS

Let us calculate the energy change ΔW (per unit length of a line perpendicular to the plane in Fig. 1(e)) that characterizes the CGBSNN process in a nanocrystalline specimen. The change ΔW is the difference in the energy between the final state [Fig. 1(e)] and initial state [Fig. 1(b)] of the system under consideration. It is convenient to represent the defect configuration consisting of five disclinations in its final state [Fig. 1(e)] as that consisting of the following three disclination dipoles: the dipole AC characterized by the strengths $\pm(\omega-\omega')$, the dipole DC characterized by the strengths $\pm\omega'$, and the dipole BE characterized by the strengths $\pm\omega'$ (Fig. 3). In doing so, the disclination C [Figs. 1(e) and 3] is represented as the superposition of the two disclinations [having the sum strength $-\omega$ in accordance with Fig. 1(e)] belonging to the dipoles AC and DC. In these circumstances, with the absence of disclinations in the initial state, the energy change ΔW can be written as follows:

$$\Delta W = W_1 + W_2 + W_3 + W_{1-2} + W_{1-3} + W_{2-3} + \Delta W_{\rm gb} - A. \tag{1}$$

Here W_1, W_2, W_3 are the proper energies of the disclination dipoles AC, DC, and BE, respectively (hereinafter indexes 1, 2, and 3 correspond to the dipoles AC, DC, and BE, respectively); W_{1-2}, W_{1-3}, W_{2-3} are the energies that characterize the elastic interaction between the disclination dipoles; $\Delta W_{\rm gb}$ is the change in the GB energy due to GB splitting that accompanies nucleation of the nanograin [Fig. 1(e)]; and A denotes the work of the external stress τ, spent to both GB sliding and GB migration. Let us designate the distance between the disclinations of the ith dipole as p_i, and the strength magnitude of the ith dipole as ω_i ($i = 1,2,3$). In this case, the proper energies W_i are given by the following standard formula:[47]

$$W_i = \frac{D\omega_i^2 p_i^2}{2}\left(\ln\frac{R}{p_i} + \frac{1}{2}\right), \quad i = 1,2,3, \tag{2}$$

where $D = G/[2\pi(1-\nu)]$, G denotes the shear modulus, ν the Poisson ratio, and R the screening length for the stress fields of the disclinations. The energy W_{i-j} ($i = 1,2$, $j = 2,3$, $i \neq j$) of the interaction between the ith and jth disclination dipoles is calculated by the standard method[50] as the work spent to the generation of one dipole in the stress field of another dipole. In doing so, after some algebra, we find the following expression for W_{i-j} ($i = 1,2$, $j = 2,3$, $i \neq j$):

$$W_{i-j} = \frac{D\omega_i\omega_j}{2}\left(L_i^2\ln\frac{R}{L_i} + L_j^2\ln\frac{R}{L_j} - L_{ij}^2\ln\frac{R}{L_{ij}} - q_i^2\ln\frac{R}{q_i} + p_i p_j\right), \tag{3}$$

where

$$\begin{aligned} L_1 &= \sqrt{p_1^2 - 2p_1q_1\sin\alpha + q_1^2}, \\ L_2 &= \sqrt{p_2^2 + 2p_2q_1\sin\alpha + q_1^2}, \\ L_3 &= \sqrt{p_3^2 + 2p_3q_1\sin\alpha + q_1^2}, \\ L_{ij} &= \sqrt{(p_j - p_i)^2 + 2(p_j - p_i)q_i\sin\alpha + q_i^2}, \\ q_1 &= \sqrt{p_2^2 + 2p_2d\cos\varphi + d^2}, \\ q_2 &= 0, \quad \alpha = \varphi - \pi/2 - \arcsin(p_1\sin\varphi/q_1). \end{aligned} \tag{4}$$

Here d denotes the length of the segment AB (Fig. 1), and the angle φ is shown in Fig. 1(b). Also, hereinafter we will approximately take d as the grain size.

The energy change $\Delta W_{\rm gb}$ [per unit length of a line perpendicular to the plane in Fig. 1(e)] is due to both the formation of the new GB DE and splitting-induced change in misorientation of the GB fragment AB. In this situation, $\Delta W_{\rm gb}$ is estimated as

$$\Delta W_{\rm gb} = \gamma_{\rm gb} d. \tag{5}$$

Here $\gamma_{\rm gb}$ is the specific energy of a tilt GB per unit of its area. In most materials the GB energy $\gamma_{\rm gb}$ versus tilt misorientation θ, for $\theta > 15^\circ$, is a slowly increasing or approximately constant function of θ with energy "cusps" associated with special GBs in some narrow intervals of θ.[51] For simplicity, we do not consider special GBs and assume $\gamma_{\rm gb}(\theta)$ to be constant. In the case of the CGBSNN process in a polycrystal (Fig. 2), $\Delta W_{\rm gb} = \gamma_{\rm gb}(d + p')$, where p' is the length of the new GB B′E′. The term $\gamma_{\rm gb}p'$ is specific for the CGBSNN process in a polycrystal (Fig. 2). Its contribution to the general energy change ΔW is typically low, in which case the energy characteristics of the CGBSNN processes

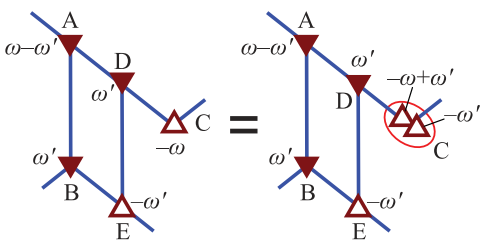

FIG. 3. (Color online) The defect configuration consisting of five disclinations is equivalent to the configuration consisting of the disclination dipole AC characterized by the strengths $\pm(\omega-\omega')$, the disclination dipole DC characterized by the strengths $\pm\omega'$ and the disclination dipole BE characterized by the strengths $\pm\omega'$.

in nanocrystalline and polycrystalline solids (Figs. 1 and 2, respectively) are very similar.

The work A of the external shear stress τ has the two terms: $A = A_1 + A_2$, where A_1 is the work spent to GB sliding [Fig. 1(c)] and A_2 is the work spent to stress-driven migration of the GB DE [Fig. 1(e)]. Let x be the magnitude of the relative displacement of grains due to GB sliding or, in other words, the distance between the GB junctions A and C. In these circumstances, we find $A_1 = \tau x d \cos 2\beta$,[29,34] where β is the angle made by the segment AC and the direction of the maximum shear stress action [Fig. 1(c)]. During the CGBSNN process, in parallel with GB sliding that causes the relative displacement of grains over the distance x, stress-driven migration of the vertical GB occurs over the distance y from its initial position AB to the new position DE [Fig. 1(e)]. Let y be the distance migrated by the GB DE [Figs. 1(e)]. With the assumption that the migrating GB DE is a symmetric tilt boundary, the work A_2 is given as $A_2 = \tau\omega' d y \sin\varphi \cos 2\beta$. Then we find

$$A = \tau d(x + \omega' y \sin\varphi)\cos 2\beta. \tag{6}$$

As a result, from formulas (1)–(6) we obtain

$$\begin{aligned}\Delta W = {} & \frac{D}{2}\sum_{i=1}^{3}\omega_i^2 p_i^2\left(\ln\frac{R}{p_i}+\frac{1}{2}\right)+\gamma_{\rm gb}d \\ & -\tau d(x+\omega y\sin\varphi)\cos 2\beta \\ & +\frac{D}{2}\sum_{i=1}^{2}\sum_{\substack{j=2\\ j\neq i}}^{3}\omega_i\omega_j\left(L_i^2\ln\frac{R}{L_i}+L_j^2\ln\frac{R}{L_j}\right. \\ & \left.-L_{ij}^2\ln\frac{R}{L_{ij}}-q_i^2\ln\frac{R}{q_i}+p_i p_j\right),\end{aligned} \tag{7}$$

where

$$\begin{aligned} & p_1 = y, \quad p_2 = x - y, \quad p_3 = x, \\ & \omega_1 = \omega_2 = \omega', \quad \omega_3 = \omega - \omega'. \end{aligned} \tag{8}$$

[In derivation of formulas (8), the previously given definitions of x, y, and ω_i are taken into account.]

Formulas (7) and (8) describe ΔW as a function of two variables x and y. In this context, it is convenient to present and analyze ΔW in terms of maps. Figure 4 shows a typical map of $\Delta W(x,y)$ written in units of $10^{-2} D\, d^2$ and calculated in the intervals of variables, $2\text{ nm} \leqslant x \leqslant d$ and $2\text{ nm} \leqslant y \leqslant x$, in the case of nanocrystalline Ni. In our calculations, we used the following typical values of material parameters of Ni: $G = 73$ GPa, $\nu = 0.34$,[52] and $\gamma_{\rm gb} = 0.866\ \text{J/m}^2$.[53] Other parameters of the system under consideration were taken as $R = 3d$, $\varphi = 2\pi/3$, $\beta = 0$, $\tau = 0.05D$, $\omega = 0.3$, $\omega' = \omega/2$, and $d = 10$ nm. The grain size is chosen as $d = 10$ nm, because commonly the GB dominated plasticity occurs in nanocrystalline Ni at room temperature when grain sizes are around and below 10–15 nm, while dislocation slip dominates in room-temperature deformation at grain sizes larger than 20 nm; see, e.g., the experiments[54–56] and a review.[17] (At the same time, there are experimental observations of GB-dominated superplasticity of nanocrystalline and ultrafine-grained Ni with widely ranging grain sizes in the temperature range 350–490°C.[22,23,25] In this context, our estimates can be extended to larger values of grain size of Ni, when its superplastic deformation at elevated temperatures is considered.)

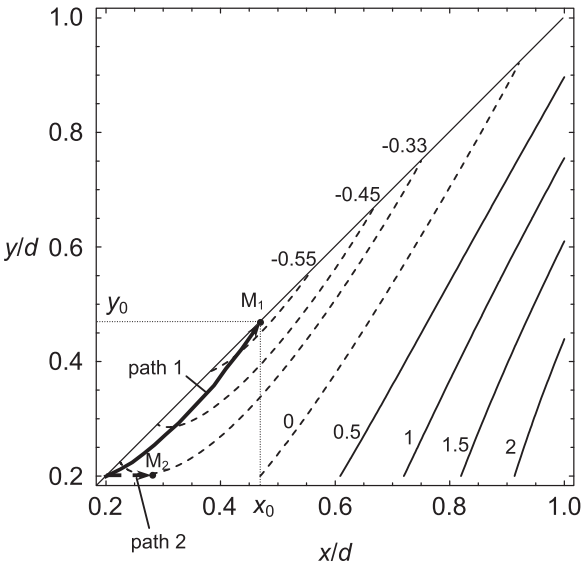

FIG. 4. Map of the energy change $\Delta W(x,y)$, calculated in the intervals of $2\text{ nm} < x \leqslant d$ and $2\text{ nm} < y \leqslant x$, in nanocrystalline Ni, for $R = 3d$, $\varphi = 2\pi/3$, $\tau = 0.05D$, $d = 10$ nm, $\omega = 0.3$, $\omega' = \omega/2$. Values of ΔW are shown in units of $10^{-2} D d^2$.

Note that the atomistic details of the GB splitting dominate at its very initial stage specified by ultralow values of the variables: x, $y < 2$ nm. To describe such details, atomistic simulations are needed that are beyond the scope of our continuum approach. At the same time, the energy profit of the GB splitting [Fig. 1(e)] in the range of $x, y \geqslant 2$ nm is critical for the splitting to occur, because the very initial stage ($x, y > 2$ nm) can be realized through thermally assisted formation of steps at the initial GB, if the splitting of the GB at $x, y \geqslant 2$ nm is energetically favorable. In this context we will focus our analysis on the situation where $x, y \geqslant 2$ nm.

Figure 4 shows a minimum (point M_1) of the energy change ΔW at some values x_0 and y_0, and the path 1 from the starting point ($x = 2$ nm, $y = 2$ nm) toward the point M_1 is characterized by the absence of any energy barrier. In these circumstances, the CGBSNN process under our examination (Fig. 1) is nonbarrier in the considered intervals: $2\text{ nm} \leqslant x \leqslant d$ and $2\text{ nm} \leqslant y \leqslant x$. From Fig. 4 it is seen that the minimum of ΔW is located at point M_1 with $x_0 = y_0$. That is, the configuration shown in Fig. 1(f) is stable.

Now let us compare the conditions for realization of (a) the CGBSNN process, (b) pure GB sliding, and (c) cooperative GB sliding and migration process. First, note that geometry of the grain structure under our analysis (Fig. 1) favors both the CGBSNN process as well as the cooperative GB sliding and migration process. This aspect is well illustrated by the process (c) in the situation where GB sliding produces the dipole of $(+\omega)$ disclination A and $(-\omega)$ disclination C, and a low-angle tilt boundary AB migrates cooperatively with GB sliding [Figs. 5(a)–5(c)]. The low-angle tilt boundary AB is modeled as a finite wall of lattice dislocations whose motion is

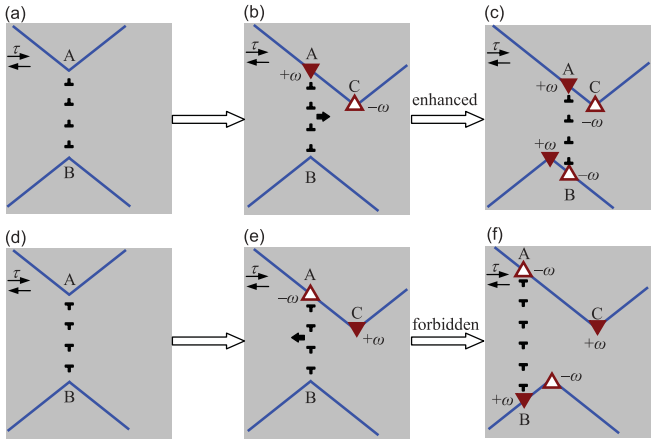

FIG. 5. (Color online) Competition between grain boundary sliding and cooperative grain boundary sliding and migration process. (a) Initial configuration of grain boundaries is presented, which enhances cooperative grain boundary sliding and migration process. Grain boundary AB is a low-angle tilt boundary that consists of periodically arranged lattice dislocations whose Burgers vectors are oriented from the left to the right. (b) GB sliding occurs, which produces the dipole of $(+\omega)$ disclination A (full triangle), and $(-\omega)$ disclination C (open triangle). (c) The shear stress τ drives the dislocations to slip to the right direction, and the low-angle tilt boundary AB migrates cooperatively with GB sliding. (d). Initial configuration of grain boundaries is presented, which enhances pure grain boundary. Grain boundary AB is a low-angle tilt boundary that consists of periodically arranged lattice dislocations whose Burgers vectors are oriented from the right to the left. (e) GB sliding occurs which produces the dipole of $(-\omega)$ disclination A (open triangle) and $(+\omega)$ disclination C (full triangle). (f) The shear stress τ drives the dislocations to slip to the left direction, but this migration is forbidden because it highly increases both the disclination strain energy as well as the length and thereby energy of the migrating boundary.

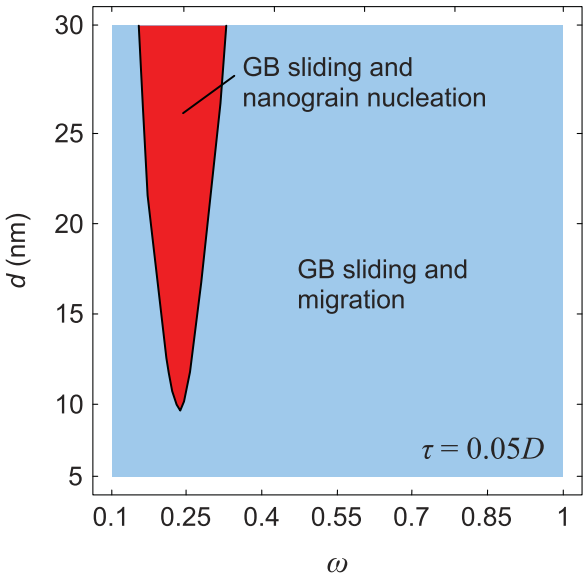

FIG. 6. (Color online) The area plot, for nanocrystalline Ni deformed at $\tau = 0.05D$, illustrating the ranges of parameters d (grain size) and ω (strength magnitude of disclinations at migrating grain boundary), where either the cooperative grain boundary sliding and nanograin nucleation process or the cooperative grain boundary sliding and migration processes dominates.

driven by the external shear stress [Figs. 5(a)–5(c)]. In addition, the migration process is driven by relaxation of the elastic energy of the disclinations involved in the process; for details, see Ref. 34.

In general, in parallel with the grain structure illustrated in Figs. 5(a)–5(c), other grain structures exist in real nanocrystalline materials. For instance, let us consider the situation [Figs. 5(d)–5(f)] where GB sliding produces the $(-\omega)$ disclination A and $(+\omega)$ disclination C [with strengths opposite to those of the disclinations shown in Figs. 5(a)−5(c)], and the dislocations of the low-angle tilt boundary AB have Burgers vectors opposite to those shown in Figs. 5(a)–5(c). In this "opposite" situation [Figs. 5(d)–5(f)], the external shear stress drives migration of the low-angle tilt boundary AB to the left direction, but this migration highly increases both the disclination strain energy and the energy of the migrating boundary (because its length should grow for geometric reasons [Fig. 5(f)]). As a corollary, in the "opposite" situation [Figs. 5(d)–5(f)], the cooperative GB sliding and migration process is suppressed, while pure GB sliding dominates. A similar "opposite" situation (where the external shear stress drives a process that, at the same time, leads to an increase in both the disclination strain energy and the GB energy) comes into play for the CGBSNN process, which is thereby suppressed, while pure GB sliding is favored. Thus, in parallel with grain structures [Figs. 1 and 5(a)–5(c)] that favor the CGBSNN process as well as the cooperative GB sliding and migration process, real nanocrystalline solids also contain grain structures [Figs. 5(d)–5(f)] whose geometry makes pure GB sliding dominate. As a corollary, all three processes under our examination—pure GB sliding, the CGBSNN process, as well as the cooperative GB sliding and migration process—can simultaneously occur in various local regions (with various grain structures) of a deformed nanocrystalline solid. In particular, pure GB sliding is enhanced in grain structures shown in Figs. 5(d)–5(f).

Now let us return to consideration of grain structures [Figs. 1 and 5(a)–5(c)] that favor the CGBSNN process as well as the cooperative GB sliding and migration process. In this situation, the CGBSNN process is energetically preferred compared to pure GB sliding [Fig. 1(c)], which corresponds to path 2 (Fig. 4) with a minimum of the energy change at point M_2. (The energy profit at point M_2 is lower than that at point M_1.) The preference is related to the definitive feature—cooperative character—of the CGBSNN process. GB sliding and nanograin nucleation effectively accommodate each other when they simultaneously carry plastic flow [Fig. 1(e)].

In Ref. 34, we theoretically examined the cooperative GB sliding and migration process. It can be treated as a partial case of the CGBSNN process, namely, the case where the GB *AB* migrates as a whole (and does not split into two GBs); see, e.g., Figs. 5(a)–5(c). In terms of disclination and GB parameters, the cooperative GB sliding and migration process is described by the relations $\omega' = \omega$ and $\Delta W_{gb} = 0$. In the situation with grain structures [Figs. 1 and 5(a)–5(c)] that favor the CGBSNN process as well as the cooperative GB sliding and migration

process, we calculated the energy maps for these processes in the coordinates/parameters (d, ω). Then we compared the maps and found the ranges of the parameters (d, ω), in which the processes under consideration are energetically preferred. Figure 6 presents the plot calculated in the exemplary case of nanocrystalline Ni at $\tau = 0.05D$, with d and ω being in the ranges: 5 nm $< d <$ 30 nm and $0.1 < \omega < 1$, respectively. In Fig. 6 we distinguished a region corresponding to the energetically favored CGBSNN process. As follows from Fig. 6, the cooperative GB sliding and migration process is more typical than the CGBSNN process (dominating in a rather narrow range of the characteristic disclination strength ω near $\omega = 0.25$).

Our calculations of the energy change for the CGBSNN process were performed in the case of $\beta = 0$, that is, the case with most favorable orientation of GBs for both GB sliding and migration leading to the nanograin nucleation. Both GB sliding and migration (Fig. 1) have the same favored direction to be enhanced by the external shear stress. Moreover, they are sensitive to the shear stress direction in the same way. In these circumstances, change in the angle β is equivalent to a change in the effective value of the shear stress (driving both GB sliding and migration leading to the nanograin nucleation; Fig. 1) in accord with formula (6). In the angle interval $45^\circ < \beta \leqslant 90^\circ$, the effective shear stress becomes negative. As a corollary, within this interval, the characteristic energy change $\Delta W > 0$ at any values of other parameters of the system, and the CGBSNN process (Fig. 1) does not occur.

IV. "STRESS-STRAIN" DEPENDENCES FOR COOPERATIVE GRAIN BOUNDARY SLIDING AND NANOGRAIN NUCLEATION PROCESS: ITS EFFECT ON INTRINSIC DUCTILITY OF NANOCRYSTALLINE SOLIDS

In recent years a particular attention has been paid to experimental results[57–60] giving evidence of enhanced tensile ductility of nanocrystalline metals without preexistent cracks and pores, because these results are indicative of intrinsic ductility of nanocrystalline structures. When a nanocrystalline solid is free from fabrication-produced cracks, its tensile ductility is limited by plastic flow localization and/or brittle crack nucleation.[18,57] In this section we will theoretically examine conditions for plastic flow localization and brittle crack nucleation in nanocrystalline materials predominantly deformed by the CGBSNN process. Also, we will compare these conditions with those for plastic flow localization and brittle crack nucleation in nanocrystalline materials predominantly deformed by either the pure GB sliding or the cooperative GB sliding and migration process.

Conditions for plastic flow localization in a solid crucially depend on its "stress-strain" curves. Therefore, for the aims of this section, we should calculate typical "stress-strain" curves for nanocrystalline materials predominantly deformed by the CGBSNN process. The process in question produces plastic flow characterized by local plastic strain $\varepsilon_{\mathrm{CGSBNN}} = \varepsilon_{\mathrm{GBS}} + \varepsilon_{\mathrm{mig}}$, where $\varepsilon_{\mathrm{GBS}}$ is the strain carried by GB sliding and $\varepsilon_{\mathrm{mig}}$ is the strain carried by GB migration. Let us estimate the strains $\varepsilon_{\mathrm{GBS}}$ and $\varepsilon_{\mathrm{mig}}$. The local plastic strain carried by GB sliding within one grain specified by the size d is given as $\varepsilon_{\mathrm{GBS}} = x_0/d$.[27] When a symmetric tilt boundary with the tilt misorientation ω' migrates, it produces the plastic strain $2\tan(\omega'/2)$ within the area swept by the migrating GB. The area swept by a GB during its migration over the distance y_0 takes the following fraction of a grain: y_0/d. In this situation the mean plastic strain within one grain is given as $\varepsilon_{\mathrm{mig}} = 2y_0\tan(\omega'/2)/d$. As a result, we find $\varepsilon_{\mathrm{CGBSNN}} = [x_0 + 2y_0\tan(\omega'/2)]/d$.

Grains in a real nanocrystalline specimen are chaotically oriented; that is, structural elements like that shown in Fig. 1(b) are specified by arbitrary orientation angles β relative to the applied stress direction. Therefore, in order to describe the plastic deformation related to the cooperative GBSNN process in a real nanocrystalline specimen, we introduce the mean plastic strain (averaged over the angle β) as follows:

$$\langle\varepsilon_{\mathrm{CGBSNN}}\rangle = (2/\pi)\int_0^{\pi/2}\{[x_0 + 2y_0\tan(\omega'/2)]/d\}d\beta, \qquad (9)$$

where x_0 and y_0 are calculated through minimization of expression (7) at given values of τ, ω, and ω'.

With formulas (7) and (9), we calculated $\langle\varepsilon_{\mathrm{CGBSNN}}\rangle$ in the exemplary situation with nanocrystalline Ni. Results of our calculations are presented in Fig. 7 as the dependence of $\langle\varepsilon_{\mathrm{CGBSNN}}\rangle$ (solid curve) on the applied stress τ, for $d = 15$ nm, $\omega = 0.25$, and $\omega' = \omega/2$ [Fig. 7(a)], and the dependence of $\langle\varepsilon_{\mathrm{CGBSNN}}\rangle$ (solid curve) on the disclination strength ω (in the case of $\omega' = \omega/2$) at $\tau = 0.8$ GPa [Fig. 7(b)]. For comparison, we calculated the same dependences for the mean plastic strains $\langle\varepsilon_{\mathrm{GBS}}\rangle$ in the case of "pure" GB sliding (dashed curves) and $\langle\varepsilon_{\mathrm{CGBSM}}\rangle$ in the case of the cooperative GB sliding and migration process (dotted curves).

The dependences $\langle\varepsilon\rangle(\tau)$ (Fig. 7) allow us to examine conditions for plastic flow instability (plastic flow localization in shear bands) in a nanocrystalline specimen deformed predominantly by either the CGBSNN process or cooperative GB sliding and migration process or pure GB sliding. In doing so, we exploit Considère's criterion (see, e.g., Ref. 57), which states that plastic flow is unstable (drastically localizes in shear bands) if $d\tau/d\varepsilon \leqslant \tau$. We performed analysis of both the dependences $\langle\varepsilon_{\mathrm{CGBSNN}}\rangle(\tau)$ calculated by formula (9) for the CGBSNN process and the dependences $\langle\varepsilon_{\mathrm{CGBSM}}\rangle(\tau)$ obtained in the same way for GB sliding and $\langle\varepsilon_{\mathrm{GBS}}\rangle(\tau)$ for the cooperative GB sliding and migration process. The analysis shows that Considère's criterion is not valid in the examined situation with nanocrystalline Ni at any values of ω for all the processes in question. Thus, in the situation where a nanocrystalline specimen is deformed predominantly by either the CGBSNN process or cooperative GB sliding and migration process or pure GB sliding, the plastic strain instability is suppressed, and plastic flow occurs homogeneously.

In the context discussed, since intrinsic ductility of nanocrystalline structures is generally limited by plastic flow localization and/or brittle crack nucleation,[18,57] the intrinsic ductility of nanocrystalline solids in the considered cases is controlled by crack nucleation. As a corollary, when a nanocrystalline solid is free from fabrication-produced cracks, its intrinsic ductility, in a first approximation, is specified by the critical plastic strain ε_c at which stable cracks nucleate in

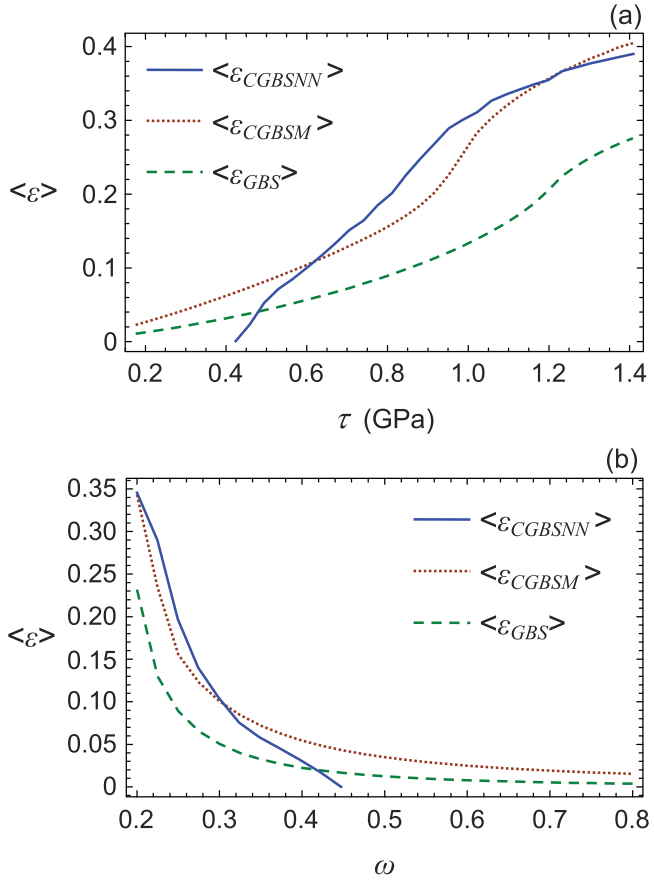

FIG. 7. (Color online) Dependences of mean plastic strain, for nanocrystalline Ni on (a) applied stress τ, for $\omega = 0.25$; and (b) disclination strength ω at $\tau = 0.8$ GPa. Other parameters are as follows: $R = 3d$, $\varphi = 2\pi/3$, $d = 15$ nm. Solid curves $\langle\varepsilon_{\text{CGBSNN}}\rangle$ correspond to the dependences in the case of the cooperative grain boundary sliding and nanograin nucleation process (with $\omega' = \omega/2$), dotted curves $\langle\varepsilon_{\text{CGBSM}}\rangle$ to the cooperative grain boundary sliding and migration process, dashed curves $\langle\varepsilon_{\text{GBS}}\rangle$ to pure grain boundary sliding.

the solid under mechanical load. Let us estimate values of ε_c in the cases of CGBSNN process resulting in configuration IV [Fig. 1(f)] and compare them to those in the cases of the cooperative GB sliding and migration process and pure GB sliding (using results obtained in.[34]) In our analysis we exploit the energy criterion[27] for triple junction crack nucleation and growth at disclination dipoles in deformed NC materials. The criterion allows one to reveal the condition at which the energetically favorable formation of a stable crack with the length l at a disclination dipole with the arm p occurs. With results,[27] the condition is as follows: $q(\tilde{l}) > q_c$. Here $\tilde{l} = l/p$,

$$q(\tilde{l}) = \tilde{l}\left\{\left[\frac{2(\sqrt{1+\tilde{l}}-1)}{\tilde{l}} - \ln\frac{\sqrt{1+\tilde{l}}+1}{\sqrt{1+\tilde{l}}-1}\right]^2 + \left[\frac{2\pi(1-\nu)\tau}{G\omega}\right]^2\right\}, \tag{10}$$

the parameter $q_c = 32\pi(1-\nu)\gamma/(Gp\omega^2)$ when a crack nucleates or grows within a grain interior [Fig. 1(d)], or $q_c = 16\pi(1-\nu)(2\gamma - \gamma_{\text{gb}})/(Gp\omega^2)$ when a crack nucleates or grows along a GB [Fig. 1(f)], γ is the specific free surface energy (per unit area), and γ_{gb} is the specific GB energy (per unit GB area) released when a crack nucleates or grows along the GB. With geometry of the grain structure presented in Fig. 1(d), in the case of pure GB sliding, the crack nucleates or grows within the grain interior because local stresses created by the disclination dipole AC are highest in this area. In the case of CGBSNN process, following our calculations [see Fig. 4(a)], a typical stable equilibrium configuration is configuration IV shown in Fig. 1(f), where both the disclination dipoles AC and BE have equal arms and strengths (with the assumption that $\omega' = \omega/2$). In doing so, a crack is evidently generated near the disclination dipole BE, and its growth occurs along the GB [Fig. 1(g)] as this process is easier due to additional release of the GB surface energy, compared to crack growth in a grain interior. Therefore, in the case of the CGBSNN process, we focus our study on crack growth along the GB [Fig. 1(g)].

In general, according to the criterion (10), the energetically favorable nucleation and growth of a crack occur when its length l is within the interval $l_1 < l < l_2$ revealed by the criterion. That is, any crack having its length within the interval grows until its length reaches the value of l_2, in which case the crack becomes stable (for details, see Refs. 27 and 61). With the above formulas, we calculated the critical value of local plastic strainε_c, at which length $l_1 \leqslant 3$ nm and $l_2 \geqslant 3$ nm; that is, a stable crack with the length of at least 3 nm is formed in a nanocrystalline Ni. In our calculation, we used $\gamma = 1.725$ J/m^2 (the value of specific surface energy in Ni,[52]) $d = 50$ nm, $\omega = 0.5$ and 0.7, $\omega' = \omega/2$. (The grain size is chosen as $d = 50$ nm, because this case well illustrates nanocrack nucleation due to GB sliding and corresponds to the experimental data[23] on the GB-dominated superplasticity exhibited by Ni with a typical grain size$d = 50$ nm in its initial, predeformation state at elevated temperatures.) For these values, in the case of the CGBSNN process [Fig. 1(g)], we found that the critical local plastic strain has value of $\varepsilon_c \approx 0.56$ at $\omega = 0.5$ and $\varepsilon_c \approx 0.26$ at $\omega = 0.7$. Moreover, when $\omega < 0.4$, the crack formation is energetically unfavorable (for the conditions specified above) at realistic values of the applied stress. In the case of pure GB sliding [Fig. 1(d)], using results of papers,[27,34] one finds $\varepsilon_c \approx 0.13$ at $\omega = 0.5$ and $\varepsilon_c \approx 0.07$ at $\omega = 0.7$. Finally, in the case of the cooperative GB sliding and migration process, with results of our previous work,[34] we find $\varepsilon_c \approx 0.18$ at $\omega = 0.5$ and $\varepsilon_c \approx 0.12$ at $\omega = 0.7$. These estimates allow us to conclude that the CGBSNN process is characterized by significantly larger values of ε_c (that specifies intrinsic ductility of nanocrystalline structures) compared to those in the cases of pure GB sliding and the cooperative GB sliding and migration process. In this context, the CGBSNN process enhances ductility of nanocrystalline and ultrafine-grained solids, and this enhancing effect is more pronounced compared to that of the cooperative GB sliding and migration process.

V. CONCLUDING REMARKS

The CGBSNN process (Figs. 1 and 2) plays the role of a special physical mode of plastic deformation in nanocrystalline, ultrafine-grained, and polycrystalline solids. Its constituent

deformation modes—GB sliding and stress-driven nanograin nucleation—effectively accommodate each other through transformations of GB disclinations. In these circumstances, in certain ranges of parameters (d,ω) of GB structures like those shown in Figs. 1 and 5(a)–5(c), the CGBSNN process is more energetically favorable than both conventional GB sliding and the previously examined[34] cooperative GB sliding and migration process in nanocrystalline solids. It is theoretically revealed that intrinsic ductility (specified by the critical plastic strain ε_c, at which a stable crack with the length at least 3 nm is formed) of a nanocrystalline Ni enhances, if the CGBSNN process dominates, compared to the situations where either pure GB sliding or the cooperative GB sliding and migration process is dominant. Results of our theoretical description of the CGBSNN process (resulting, in particular, in formation of nanoscale grains at triple junctions of GBs) are in a good agreement with the experimental observations[39–41] and computer simulations[44,45] of deformation-induced formation of new nanoscopic and microscopic grains at triple junctions of GBs in polycrystalline and nanocrystalline solids during their plastic deformation.

GB sliding plays the critical role in superplastic deformation in nanocrystalline, ultrafine-grained,[24] and polycrystalline materials.[2,12,18,24,26] Also, GB sliding significantly contributes to plastic flow of nanocrystalline materials with finest grains.[1,2,17,18,35] In all these situations, according to results of our theoretical model, the nanograin nucleation through splitting and migration of GBs can effectively accommodate GB sliding. As a corollary, the nanocrack generation is suppressed, and intrinsic ductility of materials increases.

ACKNOWLEDGMENTS

The work was supported, in part, by the Russian Ministry of Education and Science (Contract 14.740.11.0353 and Grant MK-1702.2010.1), and the Russian Academy of Sciences Program "Fundamental studies in nanotechnologies and nanomaterials."

[1] J. Schiøtz, T. Vegge, F. D. Di Tolla, and K. W. Jacobsen, Phys. Rev. B **60**, 11971 (1999).
[2] A. K. Mukherjee, Mater. Sci. Eng. A **322**, 1 (2002).
[3] I. A. Ovid'ko, Science **295**, 2386 (2002).
[4] Y. T. Zhu and T. G. Langdon, Mater. Sci. Eng. A **409**, 234 (2005).
[5] Z. Horita, K. Ohashi, T. Fujita, K. Kaneko, and T. G. Langdon, Adv. Mater. **17**, 1599 (2005).
[6] T. Shimokawa, A. Nakatani, and H. Kitagawa, Phys. Rev. B **71**, 224110 (2005).
[7] Y. H. Zhao, Y. T. Zhu, X. Z. Liao, Z. Horita, and T. G. Langdon, Appl. Phys. Lett. **89**, 121906 (2006).
[8] S. V. Bobylev, M. Yu. Gutkin, and I. A. Ovid'ko, Phys. Rev. B **73**, 064102 (2006).
[9] M. Yu. Gutkin, I. A. Ovid'ko, and N. V. Skiba, Phys. Rev. B **74**, 172107 (2006).
[10] V. Dupont and F. Sansoz, Acta Mater. **56**, 6013 (2008).
[11] A. M. Dongare, A. M. Rajendran, B. LaMattina, M. A. Zikry, and D. W. Brenner, Phys. Rev. B **80**, 104108 (2009).
[12] D. Gómez-García, E. Zapata-Solvas, A. Domínguez-Rodríguez, and L. P. Kubin, Phys. Rev. B **80**, 214107 (2009).
[13] X. L. Wu, Y. T. Zhu, Y. G. Wei, and Q. Wei, Phys. Rev. Lett. **103**, 205504 (2009).
[14] C. Deng and F. Sansoz, Phys. Rev. B **81**, 155430 (2010).
[15] J.-Y. Zhang, G. Liu, R. H. Wang, J. Li, J. Sun, and E. Ma, Phys. Rev. B **81**, 172104 (2010).
[16] D. Wolf, V. Yamakov, S. R. Phillpot, A. K. Mukherjee, and H. Gleiter, Acta Mater. **53**, 1 (2005).
[17] C. S. Pande and K. P. Cooper, Progr. Mater. Sci. **54**, 689 (2009).
[18] C. C. Koch, I. A. Ovid'ko, S. Seal, and S. Veprek, *Structural Nanocrystalline Materials: Fundamentals and Applications* (Cambridge University Press, Cambridge, England, 2007).
[19] M. Janecek, F. Louchet, B. Doisneau-Cottignies, Y. Bréchet, and N. Guelton, Philos. Mag. A **80**, 1605 (2000).
[20] P. M. Derlet and H. Van Swygenhoven, Scr. Mater. **47**, 719 (2002).
[21] F. Louchet, J. Weiss, and T. Richeton, Phys. Rev. Lett. **97**, 075504 (2006).
[22] S. X. McFadden, R. S. Misra, R. Z. Vaiev, A. P. Zhilyaev, and A. K. Mukherjee, Nature (London) **398**, 684 (1999).
[23] S. X. McFadden, A. P. Zhilyaev, R. S. Misra, and A. K. Mukherjee, Mater. Lett. **45**, 345 (2000).
[24] R. Z. Valiev and T. G. Langdon, Prog. Mater. Sci. **51**, 881 (2006).
[25] S. X. McFadden and A. K. Mukherjee, Mater. Sci. Eng. A **395**, 265 (2005).
[26] T. G. Langdon, J. Mater. Sci. **41**, 597 (2006).
[27] I. A. Ovid'ko and A. G. Sheinerman, Appl. Phys. Lett. **90**, 171927 (2007).
[28] I. A. Ovid'ko and A. G. Sheinerman, Phys. Rev. B **77**, 054109 (2008).
[29] I. A. Ovid'ko and A. G. Sheinerman, Acta Mater. **57**, 2217 (2009).
[30] A. V. Sergueeva, N. A. Mara, N. A. Krasilnikov, R. Z. Valiev, and A. K. Mukherjee, Philos. Mag. **86**, 5797 (2007).
[31] A. V. Sergueeva, N. A. Mara, and A. K. Mukherjee, J. Mater. Sci. **42**, 1433 (2007).
[32] K. A. Padmanabham and H. Gleiter, Mater. Sci. Eng. A **381**, 28 (2004).
[33] C. S. Pande and R. A. Masumura, Mater. Sci. Eng. A **409**, 125 (2005).
[34] S. V. Bobylev, N. F. Morozov, and I. A. Ovid'ko, Phys. Rev. Lett. **105**, 055504 (2010).
[35] M. Dao, L. Lu, R. J. Asaro, J. T. M. De Hosson, and E. Ma, Acta Mater. **55**, 4041 (2007).
[36] H. J. Fecht, E. Hellstern, Z. Fu, and W. L. Johnson, Met. Trans. A **21**, 2333 (1990).
[37] C. C. Koch, Rev. Adv. Mater. Sci. **5**, 91 (2003).
[38] X. Zhang, H. Wang, J. Narayan, and C. C. Koch, Acta Mater. **49**, 1319 (2001).
[39] X. Wu, N. Tao, Y. Hong, G. Liu, B. Xu, J. Lu, and K. Lu, Acta Mater. **53**, 681 (2005).
[40] H. Miura, T. Sakai, H. Hamaji, and J. J. Jonas, Scr. Mater. **50**, 65 (2004).
[41] H. Miura, T. Sakai, S. Andriawanto, and J. J. Jonas, Philos. Mag. **85**, 2653 (2005).

[42] Y. S. Li, N. R. Tao, and K. Lu, Acta Mater. **56**, 230 (2008).
[43] V. Yamakov, D. Wolf, S. R. Phillpot, A. K. Mukherjee, and H. Gleiter, Nat. Mater. **1**, 45 (2002).
[44] M. J. Demkowicz, A. S. Argon, D. Farkas, and M. Frary, Philos. Mag. **87**, 4253 (2007).
[45] A. Cao and Y. Wei, Phys. Rev. B **76**, 024113 (2007).
[46] A. E. Romanov, Eur. J. Mech. A **22**, 727 (2003).
[47] M. Kleman and J. Friedel, Rev. Mod. Phys. **80**, 61 (2008).
[48] S. V. Bobylev and I. A. Ovidko, Appl. Phys. Lett. **92**, 081914 (2008).
[49] S. V. Bobylev and I. A. Ovidko, Rev. Adv. Mater. Sci. **17**, 76 (2008).
[50] T. Mura, *Micromechanics of Defects in Solids* (Martinus Nijhoff, Dordrecht, 1987).
[51] A. P. Sutton and R. W. Balluffi, *Interfaces in Crystalline Materials* (Clarendon, Oxford, 1995).
[52] C. J. Smithells and E. A. Brands, *Metals Reference Book* (Butterworth, London, 1976).
[53] J. P. Hirth and J. Lothe, *Theory of Dislocations* (Wiley, New York, 1982).
[54] Z. Shan, E. A. Stach, J. M. K. Wiezorek, J. A. Knapp, D. M. Follstaedt, and S. X. Mao, Science **305**, 654 (2004).
[55] J. R. Trelewicz and C. A. Schuh, Appl. Phys. Lett. **93**, 171916 (2008).
[56] S. Cheng *et al.*, Phys. Rev. Lett. **103**, 035502 (2009).
[57] Y. M. Wang and E. Ma, Acta Mater. **52**, 1699 (2004).
[58] K. M. Youssef, R. O. Scattergood, K. L. Murty, J. A. Horton, and C. C. Koch, Appl. Phys. Lett. **87**, 091904 (2005).
[59] S. Cheng, E. Ma, Y. M. Wang, L. J. Kecskes, K. M. Youssef, C. C. Koch, U. P. Trociewitz, and K. Han, Acta. Mater. **53**, 1521 (2005).
[60] K. M. Youssef, R. O. Scattergood, K. L. Murty, and C. C. Koch, Scr. Mater. **54**, 251 (2006).
[61] I. A. Ovid'ko, A. G. Sheinerman, and E. C. Aifantis, Acta Mater. **56**, 2718 (2008).